Proc. Natl. Acad. Sci. USA
Vol. 93, pp. 7588–7593, July 1996
Biochemistry

Interaction of the histone $(H3\text{-}H4)_2$ tetramer of the nucleosome with positively supercoiled DNA minicircles: Potential flipping of the protein from a left- to a right-handed superhelical form

ALI HAMICHE*†, VALÉRIE CAROT*, MOHAMED ALILAT*, FILOMENA DE LUCIA*‡, MARIE-FRANÇOISE O'DONOHUE*§, BERNARD RÉVET¶, AND ARIEL PRUNELL*‖

*Institut Jacques Monod, Centre National de la Recherche Scientifique et Université Denis Diderot Paris 7, 2 place Jussieu, 75251 Paris Cédex 05, France; and ¶Laboratoire de Microscopie Cellulaire et Moléculaire, Institut Gustave Roussy, rue Camille Desmoulins, 94805 Villejuif Cédex, France

Communicated by Roger D. Kornberg, Stanford University School of Medicine, Stanford, CA, April 23, 1996 (received for review August 24, 1995)

ABSTRACT **We have studied the ability of the histone $(H3\text{-}H4)_2$ tetramer, the central part of the nucleosome of eukaryotic chromatin, to form particles on DNA minicircles of negative and positive superhelicities, and the effect of relaxing these particles with topoisomerase I. The results show that even modest positive torsional stress from the DNA, and in particular that generated by DNA thermal fluctuations, can trigger a major, reversible change in the conformation of the particle. Neither a large excess of naked DNA, nor a crosslink between the two H3s prevented the transition from one form to the other. This suggested that during the transition, the histones neither dissociated from the DNA nor were even significantly reshuffled. Moreover, the particles reconstituted on negatively and positively supercoiled minicircles look similar under electron microscopy. These data agree best with a transition involving a switch of the wrapped DNA from a left- to a right-handed superhelix. It is further proposed, based on the left-handed overall superhelical conformation of the tetramer within the octamer [Arents, G., Burlingame, R. W., Wang, B. C., Love, W. E. & Moudrianakis, E. N. (1991) *Proc. Natl. Acad. Sci. USA* 88, 10148–10152] that this change in DNA topology is mediated by a similar change in the topology of the tetramer itself, which may occur through a rotation (or a localized deformation) of the two H3-H4 dimers about their H3-H3 interface. Potential implications of this model for nucleosome dynamics *in vivo* are discussed.**

Nucleosome dynamics is a necessary requirement of DNA function in chromatin, including transcription, replication, or repair. It has long been thought to be mediated by the tripartite organization of the histone octamer, made of an $(H3\text{-}H4)_2$ tetramer bound with two H2A-H2B dimers (1). Thermodynamic studies of octamer assembly and disassembly showed that the forces holding the tetramer and dimers together are of a different nature and much stronger than the forces binding the dimers to the tetramer (1, 2), inspite of an extensive dimer–tetramer interface. This interface is disrupted in the first step of octamer disassembly.

The crystal structure of the nucleosome core particle (3), and even more so, of the histone octamer (4), subsequently confirmed this tripartite organization. Moreover, one of the H2A-H2B dimers in the crystal structure of the core particle appears significantly displaced from its original position (3), which probably reflects the effects of crystal-packing forces and the relative ease with which the dimers can move relative to the tetramer. Such dimer lability may also be important *in vivo*, as is emphasized by the observations of an H2A-H2B deficit in nucleosome cores originating from transcriptionally active chromatin (5), and of H2A-H2B exchange with the endogenous histone pool upon chromatin transcription (6–8).

The publication costs of this article were defrayed in part by page charge payment. This article must therefore be hereby marked "*advertisement*" in accordance with 18 U.S.C. §1734 solely to indicate this fact.

Here we provide evidence for a potential conformational flexibility of the $(H3\text{-}H4)_2$ tetramer, a tribute to the role of this tripartite organization of the histone octamer in nucleosome dynamics. This conformational flexibility is suggested by the observation of a similar affinity of the tetramer for negatively and positively supercoiled DNA minicircles, which apparently arises from the ability of the wrapped DNA to switch from a left- to a right-handed superhelix. This transition is found to require only modest positive torsional stress in the DNA, and can be triggered by DNA thermal fluctuations. It is further argued that such a change in DNA topology could hardly occur without a similar change in the topology of the protein itself.

MATERIALS AND METHODS

DNAs. The two 357-bp fragments originate from digests of plasmids pUC(357.4) (9) with *Bam*HI and pB357 (10) with *Taq*I, respectively. The first fragment contains a 5S RNA gene from sea urchin, whereas the second derives from plasmid pBR322, as the 359-bp fragment (11). The 354- and 351-bp fragments originate from *Taq*I digests of plasmid pB354 and pB351 (10), and have the same sequence as the above 357-bp *Taq*I fragment, except for the length differences.

Histones. Histone octamers (12) and tetramers (13) were prepared from duck erythrocyte nuclei by hydroxylapatite chromatography. The tetramer concentration was estimated from its absorbancy using $A_{230} = 2.75$ for a 1 mg/ml solution (14), and was cross-checked by comparison with the octamer using SDS/PAGE and quantitation of the bands after staining with Coomassie blue (15).

Chromatin Reconstitution. DNA minicircles were reconstituted with histones (histone to DNA weight ratio = r_w) using the "salt jump" method (12) in the presence of an excess of the plasmids in the supercoiled form from which the minicircles originate. Similar results were obtained through reconstitutions with the "salt dialysis" method (11), which involves a dialysis of the DNA–histone mixture from 2 M NaCl, without (not shown) or with urea (see Fig. 3), and the "low salt" method (11, 16) (not shown), in which histones are transferred from polyglutamic acid in 0.1 M NaCl. For the purpose of electron microscopy and histone quantitation, plasmid DNA was replaced by the same weight of the unlabeled topoisomer.

Gel Electrophoreses. Chromatin was electrophoresed at room temperature in 4% polyacrylamide [acrylamide to bisacrylamide = 30:1 (wt/wt)] gels either in 10 mM Tris·HCl (pH 7.5) and

†Present address: Laboratoire de Biologie Moléculaire Eucaryote (LBME), Université Toulouse 3, 118 route de Narbonne, 31062 Toulouse Cédex, France.
‡On leave from: Dipartimento di Chimica Organica e Biologica, University of Naples, 16 Via Mezzocannone, Naples 80134, Italy.
§Present address: U. 314, Institut National de le Santé et de la Recherche Médical, CHR Maison Blanche, 45 rue Cognacq Jay, 51092 Reims Cédex, France.
‖To whom reprint requests should be addressed.

1 mM EDTA (TE buffer) as described (11), or in 25 mM Tris, 190 mM glycine, and 1 mM EDTA (pH 8.3) (TEG buffer: this buffer is currently used for retardation gel electrophoresis; ref. 17) without buffer recirculation between upper and lower reservoirs, with similar results. Naked DNA was electrophoresed at room temperature in 5% polyacrylamide [acrylamide to bisacrylamide = 38:2 (wt/wt)] gels in 20 mM sodium acetate, 2 mM EDTA, 40 mM Tris-acetate (pH 7.8) (11), and 250 μg chloroquine per ml, except where otherwise stated. The radioactivity of the bands was quantitated in the dried gels using a phorphorimager (18).

Topoisomers and Topological Measurements. Topoisomers were prepared by circularization of the above DNA fragments, before or after ^{32}P end-labeling, in the presence of ethidium bromide or netropsin to achieve negative or positive supercoiling, respectively, and were purified by gel electrophoresis (11, 19). Topoisomers were identified by the difference in their linking number relative to the relaxed form (ΔLk) (11). ΔLk values were between −2.8 and +1.2, corresponding to superhelical densities (σ) between −0.083 and +0.035. Linking number increments associated with particle formation (ΔLk^n) were measured from the topoisomer distributions in the particle relaxation equilibria (12, 20).

Tetramer Oxidation. Tetramers were dialyzed against 2 M NaCl and 10 mM Tris·HCl (pH 7.5) to remove 2-mercaptoethanol and EDTA, and treated for 30 min at 37°C with Cu(II) (1,10-phenanthroline) (21) without extra oxygen added as H_2O2. The reaction was quenched by adding EDTA to 5-fold the Cu concentration. Tetramers were subsequently frozen into aliquots until use.

RESULTS

Supercoiling-Dependent Formation of the Tetramer-Containing Particle. The tetramer forms a well-defined particle

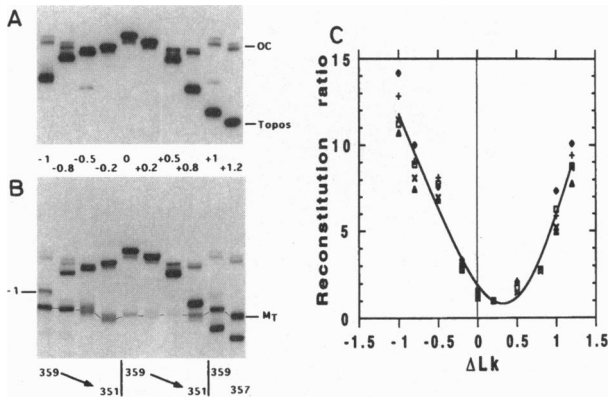

FIG. 1. Supercoiling-dependent formation of the M_T particle. Topoisomers with ΔLk = −1, 0, and +1; −0.8, +0.2, and +1.2; −0.5 and +0.5; and −0.2 and +0.8 from 359-, 357 (originating from the *Taq*I fragment)-, 354-, and 351-bp minicircles, respectively, were electrophoresed before (*A*) and after (*B*) reconstitution with $(H3\text{-}H4)_2$ tetramers (r_w = 0.6) under "chromatin gel" conditions in TE buffer. Bars join the resulting M_T bands. Autoradiograms are shown. (*C*) The fraction of each topoisomer in the M_T particle relative to total DNA in the M_T particle and residual naked topoisomer was measured from radioactivity profiles of the gel (*B*), and other similar gels derived from four additional experiments (not shown). This fraction was divided by the corresponding fraction obtained for topoisomer +0.2, and plotted as a function of ΔLk. Data were corrected, by a few percent at most, for the open circular DNA (OC), which comigrates with residual naked topoisomers −0.5, −0.2, 0, and +0.2, by excising the bands, eluting the DNAs, and measuring OC DNA relative amounts by electrophoresis in chloroquine-containing gels (see Fig. 2 *B* and *D*). A similar correction for the other topoisomers (−1, −0.8, +0.5, +0.8, +1, and +1.2) was not required because these topoisomers migrate faster than OC DNA and are not contaminated with it. Two data points are shown for topoisomer +0.8, and five for the others. The curve fit is a fifth degree polynomial.

(M_T) on both negatively and positively supercoiled DNA minicircles, as shown by the electrophoresis of a series of topoisomers before (Fig. 1*A*) and after reconstitution (Fig. 1*B*). The mobility of M_T remains approximately the same within the series, suggesting a constant histone stoichiometry (a single tetramer; see below). As shown in Fig. 1*C*, the reconstitution is about 10-fold higher on most highly supercoiled topoisomers −1 and +1.2 than on topoisomers close to relaxation (0, +0.2, +0.5), an expected reflection of the different energies required to achieve a similar compaction with all topoisomers. The increase in reconstitution with negative supercoiling (Fig. 1*C*) is not surprising since it is also observed with the octamer (11), and may simply reflect the left-handed superhelical path of the DNA on the histone surface (3, 4). The increase with positive supercoiling, in contrast, is unique to the tetramer, and points to a major departure of the wrapped DNA from its "normal" conformation.

Relaxations of M_T Particles. This normal conformation of the DNA on the tetramer surface appears to be restored upon suppression of the positive torsional stress. This is shown by topoisomerase I relaxation of the M_T particle on topoisomer +1.2, referred to below as $M_T(+1.2)$. This relaxation (Fig. 2*A*) converts all of the unreacted naked DNA into topoisomer +0.2, and generates a band containing essentially topoisomer −0.8 (Fig. 2*B*). This band comigrates with *de novo* reconstituted $M_T(-0.8)$, whose incubation with topoisomerase I has virtually no effect (not shown). This indicates that the major relaxation product of $M_T(+1.2)$ is $M_T(-0.8)$. Fig. 2*A* and *B* (lanes 4 and 6) further show that a large excess of plasmid DNA added before the relaxation fails to trap the histones. This suggests that the reversal to the normal conformation does not involve a dissociation/reassociation step of the histones.

The positive topoisomers +0.2 and +1.2 present in minor amounts in Fig. 2*B* may be true members of the M_T relaxation equilibrium. However, because the particle was assembled on the topoisomer +1.2 in the first place, the presence of this topoisomer in the relaxation products may merely be the result of an increased difficulty of the enzyme to relax the particle as compared with naked DNA. Since the relaxation equilibrium should not depend on the particular topoisomer on which the particle is first assembled (20) (at least if its' histone composition does not vary with DNA supercoiling; see above), the relaxation of $M_T(-2.8)$ should provide a better test of the possibility for topoisomer +1.2 of being a member of the equilibrium. In Fig. 2*C*, we show the effect of relaxation on the $M_T(-2.8)$ and the $M_O(-2.8)$ particles, where $M_O(-2.8)$ is the mononucleosome reconstituted from the octamer on the same topoisomer. Relaxation of M_O led to the expected equilibrium between topoisomers −1.8 and −0.8, whereas the experiment on M_T again showed, together with topoisomer −0.8, significant amounts of topoisomers +0.2 and +1.2 (Fig. 2 *D* and *E*). As will be made clear below, these positive topoisomers also signal the departure of the wrapped DNA from its normal conformation, which was already reflected in results of Fig. 1.

Associated linking number differences (ΔLk^n) were −1.2 ± 0.05 (mean ± maximal deviation for three experiments) for M_O, as previously reported (20), and −0.65 ± 0.05 for M_T. This latter value was also obtained with another 357-bp minicircle (lower profile in Fig. 2*E*), showing that the relaxation equilibrium does not depend on the DNA sequence, as expected. To show that ΔLk^n does not significantly depend on the size of the minicircles, M_T particles were also reconstituted on topoisomers −2.5 and −2 of 354- and 359-bp minicircles, respectively, and relaxed. M_T again equilibrates on both negative and positive topoisomers (Fig. 2 *F* and *G*): −0.5, +0.5, and +1.5, and −1, 0, and +1, respectively, leading to ΔLk^n = −0.5 ± 0.02 and −0.65 ± 0.02 (means ± maximal deviations for two experiments). It is interesting that these results, which show that the tetramer supercoils a DNA minicircle by about one-half the amount achieved by the octamer, are consistent with previous data showing that tetramers and octamers supercoil plasmid DNA similarly on a weight basis (22,

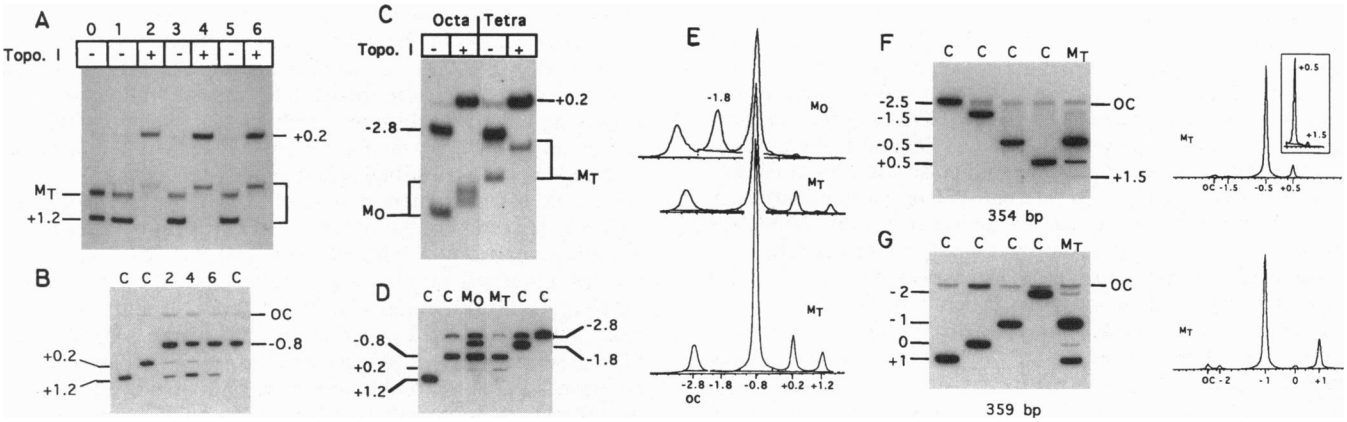

FIG. 2. Relaxation of M_T and M_O particles. (*A*) Topoisomer +1.2 of a 357-bp minicircle (originating from the *Bam*HI fragment) was reconstituted with tetramers (r_w = 0.6) and electrophoresed in TE buffer before (lane 0), and after incubation alone (lanes 1, 3, and 5) or with 600 units of topoisomerase I per ml (lanes 2, 4, and 6) under conditions previously described (12, 20). Weight excesses, 250-fold (lanes 3 and 4) and 1000-fold (lanes 5 and 6) (over total DNA) of form I pUC357.4 plasmid DNA was added prior to the incubations. Note the complete relaxation of naked topoisomer +1.2 in all + lanes. An autoradiogram is shown. (*B*) Bands in + lanes of the gel displayed in *A* were excised (bracket) and eluted DNAs were electrophoresed as naked DNAs, together with control topoisomers (lanes C). Lanes were numbered according to the lanes in *A*. OC, open circular DNA. (*C*) Topoisomer −2.8 of the same 357-bp minicircle was reconstituted with octamers (Octa; r_w = 0.4) or tetramers (Tetra; r_w = 0.3), and electrophoresed in TE buffer after incubation alone (Topo. I−) or with 300 units of the topoisomerase per milliliter (Topo. I+). Note the spreading of the M_O band after relaxation, which is due to nucleosome position-dependent fractionation (10, 18). (*D*) Bands in + lanes of the gel displayed in *C* were excised (brackets) and eluted DNAs electrophoresed. (*E*) Radioactivity profiles of M_O and M_T lanes of the gel shown in *D* (top two profiles). The lower profile corresponds to a similar relaxation experiment with topoisomer −2.8 of the 357-bp minicircle used in Fig. 1. OC, open circular DNA. (*F* and *G*) Same as *D* and *E* for the relaxation of M_T(−2.5) and M_T(−2) on 354- and 359-bp minicircles, respectively (not shown), except that the reconstituted chromatins were initially electrophoresed in TEG buffer. The captioned profile in *F* is enlarged relative to the main profile to better show topoisomer +0.5 and +1.5 proportions.

23). Finally, it is noteworthy that, among the positive topoisomers observed in the M_T equilibria, +0.2 (Fig. 2 *A* and *C*) and +0.5 (Fig. 2*F*) are also produced upon relaxation of the naked minicircles (20), whereas +1.2 (Fig. 2 *B*, *D*, and *E*), +1.5 (Fig. 2*F*), and +1 (Fig. 2*G*) are specific to M_T.

Inter H3 Crosslinking Through a Disulfide Bridge Does Not Prevent the Transition. Previous work has shown that an octamer containing H3s crosslinked by a disulfide bridge can assemble into apparently normal nucleosomes (24). This has pointed to a location of the two H3 cysteines (at position 110) on the nucleosome dyad axis, which has been confirmed by fluorescence (25) and crystallographic studies (26). Consistent with this observation, the M_T particle formed on topoisomer −1 with a tetramer containing 100% dimerized H3 (Fig. 3*B*; lane C2) resembles that obtained with the normal tetramer (Fig. 3*B*; lane C1) (compare lanes 4 and 5 with lane 1 in Fig. 3*A*). This similarity extends to topoisomers 0 and +1 (lanes 2, 3, and 6–9 in Fig. 3*A*). A low reconstitution on topoisomer 0 and a reconstitution ratio between topoisomers −1 and +1 of about 2:1 are observed with both control and oxidized tetramers (see Fig. 1*C*).

The tetramer is incorporated in the oxidized form, and there is no subsequent reduction of the S–S bridge, as can be demonstrated by second-dimension electrophoresis of the excised bands in an SDS-containing gel (Fig. 3*B*, lanes 2 and 4). The S–S bridge has no effect on the transition, as is made clear by second-dimension electrophoresis of particles reconstituted with a 1:1 mixture of normal and oxidized tetramers (Fig. 3*B*, lanes 1 and 3), which shows the same proportions of the two tetramer forms as in the control (Fig. 3*B*, lane C3). Moreover, relaxation of the M_T particle reconstituted with the oxidized tetramer on topoisomer −2 of the 359-bp minicircle leads to an equilibrium (not shown) virtually identical to that displayed in Fig. 2*G*.

Electron Microscopic Visualization. H2A-H2B dimers are not incorporated when nucleosome reconstitution is attempted on a positive topoisomer. While the topoisomer −1 gives rise to both M_O and M_T when reconstituted with the octamer and the tetramer, respectively, the topoisomer +1 leads only to M_T (Fig. 4*A*). This result shows that the normal affinity of H2A-H2B dimers for the tetramer is abolished in the presence of positive torsional stress, and is also in keeping with the known sequential deposition onto the DNA of the tetramer first and H2A-H2B

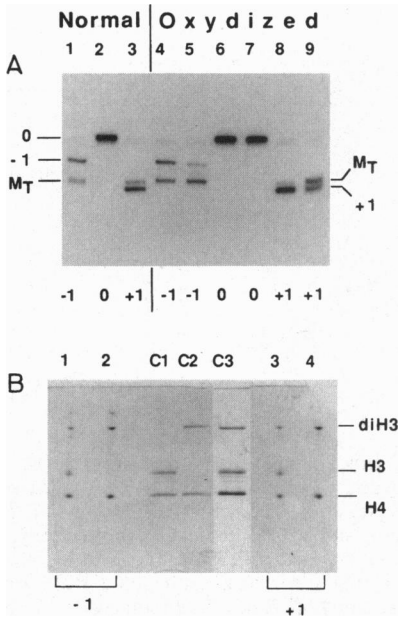

FIG. 3. M_T particle formation with the oxidized tetramer. (*A*) Topoisomers −1, 0, and +1 from Fig. 1 were reconstituted with normal (r_w = 0.15, lanes 1–3) and oxidized tetramers (r_w = 0.15, lanes 4, 6, and 8; and r_w = 0.3, lanes 5, 7, and 9) in the absence of extraneous carrier DNA, using the "salt dialysis" procedure in the presence of 5 M urea, as described (24), and electrophoresed in TEG buffer. An autoradiogram of the gel is shown. Topoisomers are indicated. (*B*) Electrophoresis in an SDS-containing polyacrylamide gel (15) of normal (C1), oxidized (C2), and normal plus oxidized tetramers (C3), and of M_T bands cut out of the gel shown in *A* (lanes 2 and 4), and of another gel displaying reconstitutions of the same topoisomers with the C3 mixture (not shown) (lanes 1 and 3). Topoisomers on which M_T particles were initially reconstituted are indicated. A photograph of the gel stained with Coomassie blue is shown. Histones are indicated. diH3, dimerized H3.

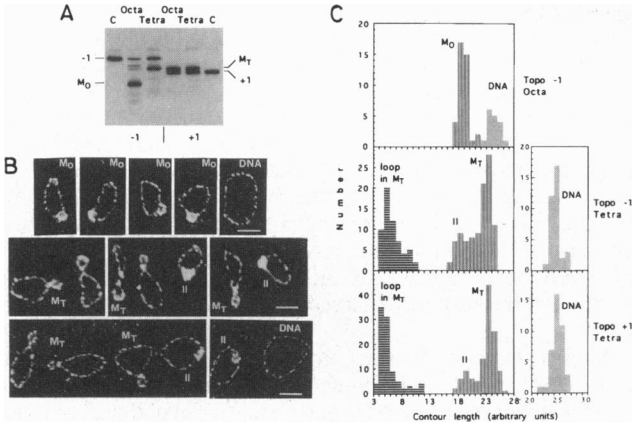

FIG. 4. Particle electron microscopic visualization. (*A*) Topoisomers −1 and +1 from Fig. 1 were reconstituted with normal (reduced) octamers (Octa) and tetramers (Tetra) at $r_w = 0.2$ in the absence of extraneous carrier DNA, and electrophoresed in TE buffer, along with naked topoisomers (*C*). An autoradiogram is shown. (*B*) Reconstitution products shown in *A* were diluted in TE buffer, adsorbed to the grids, and examined under the electron microscope as described (11). Representative molecules are shown. Top, middle, and bottom galleries: topoisomer −1 reconstituted with octamers and tetramers, and topoisomer +1 reconstituted with tetramers, respectively. Naked topoisomers (DNA), M_O, M_T, and type II particles are indicated. Typical percentages were 30–35%, 50%, and 15–20% for DNA, M_T, and type II particles, respectively, for both topoisomers −1 and +1. (Bars = 20 nm ≈60 bp.) (*C*) Contour lengths were measured using a scanner (Onescanner, Apple) and the KALEIDAGRAPH (Synergy Software, Reading, PA) software on an Apple Macintosh computer. Means of naked DNA measured on 17, 35, and 39 minicircles were at 24.4, 24.3, and 24.6 length units in the top, middle, and lower histograms, respectively, leading to a 14.7 (± 0.1) (359/24.3 to 24.6) bp per unit. Data originate from 41 M_O particles (top histogram), and 102 and 121 M_T-plus-type II particles (middle and bottom histograms, respectively). Data for 60 and 95 small loops in M_T (middle and bottom histograms, respectively) are also shown. M_O has a contour length deficit of 82 bp relative to naked DNA (as measured from the peak median values), in agreement with the 83 bp expected (3), and type II particles of 88 bp (topoisomer −1) and 73 bp (topoisomer +1). In contrast, the M_T contour length deficit is only 15 bp.

second in the nucleosome reconstitution process (27, 28). Second-dimension electrophoresis of excised M_O and M_T bands in an SDS-containing polyacrylamide gel, as performed in Fig. 3*B*, revealed equal stoichiometries of H3 and H4 in M_T, and H3, H4, H2A, and H2B in M_O (not shown). This, together with sucrose gradient sedimentations that showed M_T sedimenting half-way between M_O and naked DNA (not shown), indicates that M_T contains a single tetramer.

Electron microscopy of samples shown in Fig. 4*A* reveals a single crossing of the DNA delimiting a small, hollow, loop in both $M_T(-1)$ and $M_T(+1)$ (Fig. 4*B*; median and lower galleries). In contrast, fields of naked topoisomers −1 and +1 observed under identical conditions always display uncrossed molecules (not shown) (see, for example, the naked topoisomers in higher and lower galleries of Fig. 4*B*). This small loop therefore is likely to contain the histones, whereas the large loop is presumably naked DNA. This appearance is not salt-dependent, at least in the range from 10 mM (Fig. 4*B*) to 50 mM (not shown). Other particles (type II) are also observed in minor amounts, very similar to $M_O(-1)$ shown for comparison in upper gallery (Fig. 4*B*). Type II particles may contain two (or more) tetramers stacked on top of one another, as suggested by the previously noted tendency of tetramers to assemble limited oligomers in the absence of DNA, through interactions between their surfaces normally capped by H2A-H2B (2). Particles similar to normal nucleosomes and composed of two stacked tetramers have also been observed as a result of a sliding together of (H2A-H2B)-depleted native nucleosomes (29). M_T has a contour length similar to that of naked DNA, in contrast to M_O and type II particles, which contain a hidden DNA turn (Fig. 4*C*). A small loop of 80–88 bp and a crossing angle of 60–90° result in 53–66 [(80 to 88)(180 + 60 to 90)/360] bp wrapped into 0.67–0.75 [(180 + 60 to 90)/360] turn in both $M_T(-1)$ and $M_T(+1)$. This is in keeping with the ≈70-bp protection against micrococcal nuclease observed by us (M.A. and A.P., unpublished results) and by others (30, 31).

DISCUSSION

DNA Conformation. Tetramer affinity for DNA has been observed to increase not only with negative but also positive supercoiling (Fig. 1 *B* and *C*). The following considerations argue for this result to reflect a switch of the tetramer-bound DNA from a left-handed to a right-handed form. First, let us consider the DNA conformation in $M_T(-1)$, the complex of the tetramer with topoisomer −1. Electron microscopy revealed that DNA wraps in this particle into 0.67–0.75 turn of a presumably left-handed superhelix (Fig. 4 *B* and *C*), a figure at variance with footprinting and physico-chemical results in the literature (30–32) and our own footprinting data (A. Sivolob and A.P., unpublished data), which indicate a wrapping of at least 1.5 turns upon tetramer reconstitution on linear DNA. This low wrapping is likely to correspond to an attempt to minimize the free energy of DNA bending within the topological constraints of a DNA minicircle. Further wrapping would decrease the size of the loop and its mean radius of curvature, and increase the free energy of DNA bending. Assuming that the DNA superhelix around the tetramer has the same pitch as in the nucleosome, this leads to a writhing of the minicircle in the relaxed particle, Wr, of −0.8. This value was computed from a model of the nucleosome in which a DNA minicircle was partially wrapped around a cylindrical histone core, and the other part let free to fluctuate both in torsion and flexion (20, 33). This −0.8 figure turns out to be close to the mean linking number difference ($<\Delta Lk> = -0.77$) of topoisomers −0.8, −0.5, and −1 obtained here as M_T major relaxation products (Fig. 2). This −0.8 figure should therefore give the linking number difference, ΔLk^n, associated with formation of a potential transition-free M_T particle (ΔLk^n of the actual particle— ≈−0.6; see *Results*—originates from the occurrence of positive topoisomers in the equilibrium as a consequence of the transition). Making $\Delta Lk^n \approx Wr$ in the equation $\Delta Lk^n = \Delta Tw + Wr$ (34–36), it comes $\Delta Tw \approx 0$. In other words, the twist of the DNA, Tw, may remain essentially unaltered upon wrapping around the tetramer, as previously reported for wrapping around the octamer in the absence (20) or presence of H5 (12).

If this DNA left-handed conformation around the tetramer were to be preserved in $M_T(+1)$, ΔLk of the topoisomer would add to $|\Delta Lk^n|$, instead of subtracting as in $M_T(-1)$, generating a linking number difference in the loop ($\Delta Lk - \Delta Lk^n$) of +1.8. Such a large positive linking difference would preclude reconstitution in the first place, as observed for the nucleosome on the same topoisomer +1 (Fig. 4*A*). This linking difference has therefore to be relieved, and this can be achieved in two ways. (*i*) The DNA keeps its left-handedness, but overtwists on the tetramer surface. A simple calculation, not detailed here, shows that the relief of only one-half of the loop linking difference would require the wrapped DNA to adopt an helical periodicity of only 9 bp per turn. (*ii*) A more realistic possibility, therefore, is that the DNA switches to a right-handed superhelical path, while keeping its twist more or less unaltered. This suggests that the crossing observed in $M_T(+1)$ under the electron microscope (Fig. 4*B*; bottom) is positive, a feature that could possibly be confirmed by other techniques, such as atomic force or cryoelectron microscopies.

Interestingly, a somewhat similar conclusion was previously reached from an investigation of the influence of positive stress on nucleosome assembly (37). Reconstitution on positively supercoiled DNA was found to result in "open" structures, which, from the criterion of time- and temperature-dependent relaxation

with topoisomerase I, appeared unable to store negative coils in the way nucleosomes on negatively supercoiled DNA did. A lack of change in the DNase I cleavage periodicity led the author to suggest an alteration in the conformation of the DNA superhelix in these structures as opposed to an overtwisting of the DNA (see above) (37). Subsequently, however, the overtwisting model was preferred, based on the observation of a preference of the tetramer to bind DNA of moderate positive supercoiling (σ = +0.01) over DNA of negative supercoiling (σ = −0.05) at high ionic strength (38), this preference being maintained at physiological ionic strength for DNA of high positive supercoiling ($\sigma >$ +0.1) (39). It was argued that both salt and positive supercoiling overtwisted the DNA, which facilitated binding by relieving the histones from doing so, in agreement with the general credence that DNA is overtwisted on the nucleosome surface (but see above) (39). Although this binding preference is fully consistent with the data in Fig. 1, it should be realized that the plasmid system used in that work (37–39) is significantly more complex than the present minicircle system. In particular, the number of particles reconstituted, their exact content (tetramer or pseudo-octamer of two stacked tetramers; see *Results*), as well as the DNA path around them, could not be determined (37–39). Moreover, potential interactions between these particles, and especially tetramer-containing particles (ref. 2; see also *Results*), may bias the relaxation data by sequestering the linker DNA in between. For example, evidence for such interactions as being the reason for the unexpectedly low ability of DNA in plasmid-reconstituted nucleosomes to untwist upon an elevation of the temperature (40, 41) was recently obtained from experiments with minicircles (10).

Energetic and Dynamic Aspects. Fig. 1*C* shows that M_T reconstitution increases immediately with negative ΔLk values, as expected, whereas the increase with positive values is delayed and starts only at $\Delta Lk \approx +0.5$. This suggests that the DNA transition requires a minimal energy that can be estimated from the free energy of supercoiling, ΔG_s, of topoisomer +0.5 (σ = +0.015), approximately 1.5 kcal/mol ($\Delta G_s = A\,\Delta Lk^2$, with A = 6 kcal/mol for the present ≈350-bp minicircles; ref. 42). Beyond topoisomer +0.5, reconstitution increases with positive supercoiling at approximately the same rate as with negative supercoiling (Fig. 1*C*). This suggests that all positive topoisomers use the same fraction (≈1.5 kcal/mol) of their supercoiling energy to trigger the transition, the remaining energy serving to promote DNA wrapping, as observed in the negative branch of the curve (Fig. 1*C*). Since the transition is spontaneously reversible (Fig. 2*A*), an interesting question concerns the residual value of ΔLk required to maintain the alternative DNA conformation. This ΔLk value could be significantly smaller than the value required to trigger it, as suggested by the crossed appearance of $M_T(+1)$ under electron microscopy, which indicates that most of the topoisomer initial ΔLk went into writhe (assuming this crossing is indeed positive; see above).

The presence of positive topoisomers in M_T relaxation equilibria (Fig. 2) indicates that DNA thermal fluctuations in the loop can, at least at their peak level, trigger the transition. This is in keeping with the relatively low energy estimated above for the transition: 1.5 kcal is only 2.5 times RT, the mean DNA thermal fluctuation energy. Given the dynamic nature of the relaxation equilibrium, which implies that the various forms continuously interconvert (20), this means that the DNA fluctuates rapidly between left-handed and right-handed conformations. The lower amounts of the positive topoisomers relative to the negative topoisomers then simply reflect the higher free energy of the alternative conformation.

Protein Conformation. Although no direct information was derived from the protein, it is interesting to discuss the possible fate of the tetramer during the DNA transition. First, a change in its structure may occur through histone reschuffling (we have shown that histones are present as a tetramer on both negative and positive topoisomers; see *Results*). Three observations argue against this possibility: (*i*) the ability of the transition to occur back and forth rapidly, as demonstrated by the coexistence of negative and positive topoisomers in M_T relaxation equilibria (see above and Fig. 2); (*ii*) the lack of an excess of naked DNA to trap the histones during reversal of the transition (Fig. 2*A*); and (*iii*) the failure of a disulfide bridge crosslink between the two H3s to inhibit the transition (Fig. 3). Alternatively, the DNA may switch from one configuration to the other by slippage on a rigid histone surface. This possibility appears also unlikely in view of the crystal structure of the octamer at 3.1 Å, which shows a unique path of the DNA on its surface, as indicated by the linearly ordered positions of the positively charged basic amino acid residues along it (43).

A third possibility remains, that the change in the handedness of the DNA superhelix is somehow mediated by a similar change in the handedness of the tetramer itself. This hypothesis, as weird as it may look at first, becomes particularly appealing when the overall shape of the tetramer within the octamer crystal structure is considered (4). This tetramer actually resembles a twisted horseshoe forming a 0.75 turn of a proteinaceous left-handed molecular superhelix, with a large cavity in its center. [The DNA in $M_T(-1)$ must then simply follow the path of this protein superhelix (see above).] The left handedness of this superhelix is further described as resulting from the clockwise rotation of the two crescent-shaped H3-H4 dimers relative to each other around their H3-H3 interface (4). A highly schematic view of such tetramer overall shape is displayed in Fig. 5 (*Left*).

We propose that the two H3-H4 dimers can somehow rotate in the reverse, counterclockwise direction around their H3-H3 interface (around the S–S bridge when oxidized), and form a right-handed molecular superhelix (Fig. 5, *Right*). This rotation may be accomplished through local deformation of the structure in the dyad region. A change in protein topology is strongly supported by our recent data (unpublished) revealing an inhibition of the transition by steric hindrance at the dyad. Steric hindrance was obtained by covalent binding of bulky adducts to H3 cysteine within the tetramer or the octamer through oxidation with thiol-specific reagents such as N-ethylmaleimide (44), 5,5′-

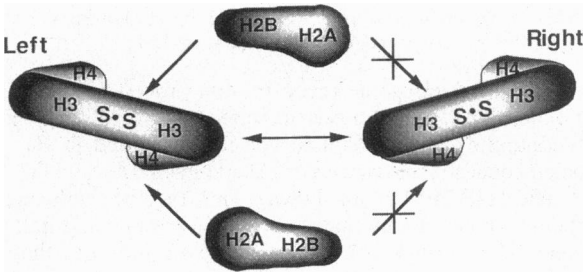

FIG. 5. Model for the proposed change in tetramer topology. (*Left*) Highly schematical representation of the $(H3\text{-}H4)_2$ tetramer overall shape within the octamer. The tetramer resembles a shallow 0.75-turn horseshoe, made of two crescent-shaped sectors (the two H3-H4 dimers), which overlap each other on the dyad axis (dot), forming a small H3-H3 interface. Each sector is off the dyad-containing plane by about 15° in the clockwise direction, generating a left-handed proteinaceous molecular superhelix (4). The S on each side of the dot figures the thiol group (SH) of H3 unique cysteine at position 110. SH are located on the dyad and are close enough (25, 26) to form a disulfide (S–S) bridge upon oxidation (ref. 24 and this work). It should be noted that the figure only shows the position of the maximal density of each histone. In the real structure, H3 and H4 polypeptides are partially intermingled so that some regions of H4 are closer to the dyad than depicted. (*Right*) Each sector was rotated around the H3-H3 interface, or the S–S bridge in the oxidized tetramer, in the counterclockwise direction, to form a right-handed molecular superhelix. In this model, this rotation requires positive torsional stress in the DNA (not shown) to be triggered and maintained (see text). The conformations shown are mirror-symmetric, which need not be the case in reality. H2A-H2B dimers can cap the left-handed tetramer to assemble an octamer, but not the right-handed tetramer (see Fig. 4*A*).

dthiobis(2-nitrobenzoic acid (DTNB) (Ellman's reagent, ref. 45), or monobromobimane (46). Consistently, subsequent reduction with 2-mercaptoethanol of the DTNB-treated material restored the flexibility. Short of crystals of tetramers (47) in their alternative conformation, atomic coordinates (4) may be used to model how the tetramer could sustain such deformation.

A Physiological Role for the Transition? The advantage of an $(H3\text{-}H4)_2$ tetramer with an affinity for positively supercoiled DNA has been extensively commented upon (37–39). Such a tetramer could sustain the positive supercoiling wave generated in front of the polymerase (48) and remain on the DNA, whereas H2A-H2B would be destabilized and released, in agreement with the observed exchange of H2A-H2B (but not of H3-H4) during transcription (6–8). This tetramer could then serve as a nucleation site for the efficient regeneration of the nucleosome under the negative supercoiling wave generated in the wake of the polymerase (38, 39). The model in Fig. 5 proposes that tetramer affinity for positive supercoiling is mediated by its ability to change its overall topology. Such potential conformational flexibility may be important not only for transcription elongation but also in transcription initiation. A possible scenario could be as follows. After H2A-H2B displacement by transacting factors, as often suggested, other factors may be recruited that could trigger tetramer transition possibly in an ATP-driven reaction. An intriguing candidate for this is the ubiquitous transcriptional activator SWI/SNF complex (49), whose defect in swi/snf yeast mutants can be partly suppressed by compensatory mutations in genes for histones H3 and H4 (50, 51). Because these mutations are single amino acid substitutions clustered around the tetramer dyad axis (52), they may affect (increase) tetramer flexibility. Moreover, the SWI/SNF complex was recently shown to have a positive DNA supercoiling activity in the presence of bacterial topoisomerase I (53), also consistent with such a role. The activator protein would behave, in triggering the transition, like a "eucaryotic-gyrase," and would elicit almost two turns of unconstrained negative supercoiling which, in the absence of local topoisomerase relaxing activity, could unwind the double helix and facilitate binding of the polymerase or other regulatory proteins. Interestingly, such transcription elongation-independent negative supercoiling, which was thought to result from the removal or modification of nucleosomes, has recently been localized to the promoter region of the transcriptionally poised dihydrofolate reductase gene *in vivo* (54). It is noteworthy that nucleosome removal would be only about one-half as efficient as the proposed mechanism in generating local negative supercoiling.

We are grateful to Mrs. B. Hermier and H. Baugier for excellent technical assistance. A.P. wishes to thank Dr. M. Le Bret (Villejuif) for discussions and Dr. V. Ramakrishnan (University of Utah School of Medicine, Salt Lake City) for a careful reading of the manuscript. V.C., A.H., and F.D.L. were supported by 1-year fellowships from the Association pour la Recherche sur le Cancer at successive stages of this work.

1. Eickbush, T. H. & Moudrianakis, E. N. (1978) *Biochemistry* **17,** 4955–4964.
2. Baxevanis, A. D., Godfrey, J. E. & Moudrianakis, E. N. (1991) *Biochemistry* **30,** 8817–8823.
3. Richmond, T. J., Finch, J. T., Rushton, B., Rhodes, D. & Klug, A. (1984) *Nature (London)* **311,** 532–537.
4. Arents, G., Burlingame, R. W., Wang, B. C., Love, W. E. & Moudrianakis, E. N. (1991) *Proc. Natl. Acad. Sci. USA* **88,** 10148–10152.
5. Baer, B. W. & Rhodes, D. (1983) *Nature (London)* **301,** 482–488.
6. Louters, L. & Chalkley, R. (1985) *Biochemistry* **23,** 3080–3085.
7. Schwager, S., Retief, J. D., de Groot, P. & von Holt, C. (1985) *FEBS Lett.* **189,** 305–309.
8. Jackson, V. (1990) *Biochemistry* **29,** 719–731.
9. O'Donohue, M. F., Duband-Goulet, I., Hamiche, A. & Prunell, A. (1994) *Nucleic Acids Res.* **22,** 937–945.
10. Hamiche, A. & Prunell, A. (1992) *J. Mol. Biol.* **228,** 327–337.
11. Goulet, I., Zivanovic, Y., Prunell, A. & Révet, B. (1988) *J. Mol. Biol.* **200,** 253–266.
12. Zivanovic, Y., Duband-Goulet, I., Schultz, P., Stofer, E., Oudet, P. & Prunell, A. (1990) *J. Mol. Biol.* **214,** 479–495.
13. Simon, R. H. & Felsenfeld, G. (1979) *Nucleic Acids Res.* **6,** 689–696.
14. Thomas, J. O. & Butler, P. J. G. (1977) *J. Mol. Biol.* **116,** 769–781.
15. Thomas, J. O. & Kornberg, R. D. (1978) *Methods Cell Biol.* **18,** 429–440.
16. Stein, A., Whitlock, J. P. & Bina, M. (1979) *Proc. Natl. Acad. Sci. USA* **76,** 5000–5004.
17. Antoniewski, C., Laval, M., Dahan, A. & Lepesant, J.-A. (1994) *Mol. Cell. Biol.* **14,** 4465–4474.
18. Duband-Goulet, I., Carot, V., Ulyanov, A. V., Douc-Rasy, R. S. & Prunell, A. (1992) *J. Mol. Biol.* **224,** 981–1001.
19. Zivanovic, Y., Goulet, I. & Prunell, A. (1986) *J. Mol. Biol.* **192,** 645–660.
20. Zivanovic, Y., Goulet, I., Révet, B., Le Bret, M. & Prunell, A. (1988) *J. Mol. Biol.* **200,** 267–285.
21. Careaga, C. L. & Falke, J. J. (1992) *J. Mol. Biol.* **226,** 1219–1235.
22. Camerini-Otero, R. D. & Felsenfeld, G. (1977) *Nucleic Acids Res.* **5,** 1159–1181.
23. Bina-Stein, M. & Simpson, R. T. (1977) *Cell* **11,** 609–618.
24. Camerini-Otero, R. D. & Felsenfeld, G. (1977) *Proc. Natl. Acad. Sci. USA* **74,** 5519–5523.
25. Daban, J. R. & Cantor, C. R. (1982) *J. Mol. Biol.* **156,** 771–789.
26. Wang, B.-C., Rose, J., Arents, G. & Moudrianakis, E. N. (1994) *J. Mol. Biol.* **236,** 179–188.
27. Wilhelm, F. X., Wilhelm, M. L., Erard, M. & Daune, M. P. (1978) *Nucleic Acids Res.* **5,** 505–521.
28. Ruiz-Carrillo, A. & Jorcano, J. L. (1978) *Cold Spring Harbor Symp. Quant. Biol.* **42,** 165–170.
29. Read, C. M. & Crane-Robinson, C. (1985) *Eur. J. Biochem.* **152,** 143–150.
30. Read, C. M., Baldwin, J. P. & Crane-Robinson, C. (1985) *Biochemistry* **24,** 4435–4450.
31. Dong, F. & van Holde, K. E. (1991) *Proc. Natl. Acad. Sci. USA* **88,** 10596–10600.
32. Hayes, J. J., Clark, D. J. & Wolffe, A. P. (1991) *Proc. Natl. Acad. Sci. USA* **88,** 6829–6833.
33. Zhang, P., Tobias, I. & Olson, W. K. (1994) *J. Mol. Biol.* **242,** 261–280.
34. White, J. H. (1969) *Am. J. Math.* **91,** 693–727.
35. Fuller, F. B. (1971) *Proc. Natl. Acad. Sci. USA* **68,** 815–819.
36. Crick, F. H. C. (1976) *Proc. Natl. Acad. Sci. USA* **73,** 2639–2643.
37. Jackson, V. (1993) *Biochemistry* **32,** 5901–5912.
38. Jackson, S., Brooks, W. & Jackson, V. (1994) *Biochemistry* **33,** 5392–5403.
39. Jackson, V. (1995) *Biochemistry* **34,** 10607–10619.
40. Morse, R. H. & Cantor, C. R. (1985) *Proc. Natl. Acad. Sci. USA* **82,** 4653–4657.
41. Morse, R. H. & Cantor, C. R. (1986) *Nucleic Acids Res.* **14,** 3293–3310.
42. Horowitz, D. S. & Wang, J. C. (1984) *J. Mol. Biol.* **173,** 75–91.
43. Arents, G. & Moudrianakis, E. N. (1993) *Proc. Natl. Acad. Sci. USA* **90,** 10489–10493.
44. Riordan, J. F. & Vallee, B. L. (1972) *Methods Enzymol.* **25,** 449–456.
45. Habeeb, A. F. S. A. (1972) *Methods Enzymol.* **25,** 457–464.
46. Kosower, E. M. & Kosower, N. S. (1995) *Methods Enzymol.* **251,** 133–148.
47. Lattman, E., Burlingame, R., Hatch, C. & Moudrianakis, E. N. (1982) *Science* **216,** 1016–1018.
48. Liu, L. F. & Wang, J. C. (1987) *Proc. Natl. Acad. Sci. USA* **84,** 7024–7027.
49. Carlson, M. & Laurent, B. C. (1994) *Curr. Opin. Cell Biol.* **6,** 396–402.
50. Winston, F. & Carlson, M. (1992) *Trends Genet.* **8,** 387–391.
51. Wolffe, A. P. (1994) *Curr. Opin. Cell Biol.* **4,** 525–528.
52. Kruger, W., Peterson, C. L., Sil, A., Coburn, C., Arents, G., Moudrianakis, E. N. & Herskowitz, I. (1995) *Genes Dev.* **9,** 2770–2779.
53. Quinn, J., Fyrberg, A. M., Ganster, R. W., Schmidt, M. C. & Peterson, C. L. (1996) *Nature (London)* **379,** 844–846.
54. Ljungman, M. & Hanawalt, P. C. (1995) *Nucleic Acids Res.* **23,** 1782–1789.